Journal of Materials Chemistry A

Accepted Manuscript

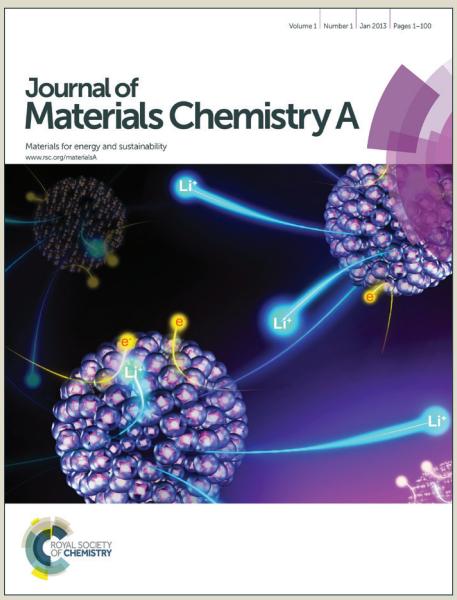

ROYAL SOCIETY OF CHEMISTRY

www.rsc.org/materialsA

Journal of Materials Chemistry RSCPublishing

PAPER

Correlation between nanoparticle location and graphene nucleation in chemical vapour deposition of graphene

Cite this: DOI: 10.1039/xoxxoooooox

Received ooth January 2014,
Accepted ooth January 2014

DOI: 10.1039/xoxxoooooox

www.rsc.org/

Lili Fan[a], Kunlin Wang[a], Jinquan Wei[a], Minlin Zhong[a], Dehai Wu[b], Hongwei Zhu*[a,c]

Nanoparticles are ubiquitously existent on the surface of graphene films prepared by chemical vapour deposition. However, studies to thoroughly explore this phenomenon are still fairly limited. In this work, we have demonstrated that the location of nanoparticles should be a straightforward reflection for the nucleation sites of graphene growth. Plus, the deposition of the nanoparticles is consistent with the distribution of multilayer graphene. We have found that nanoparticles are not nucleation seeds as proposed by other groups; instead, they are sediment-like material similar to the graphene films prepared on the copper substrates.

Introduction

Nowadays, the large-scale synthesis of high quality single-crystalline graphene has attracted great interest,[1-10] presumably because the disruption caused by grain boundaries[11,12] can be avoided in such material. Notably, single-crystalline graphene has reached centimetre scale, and its carrier mobility is up to 30000 cm^2 V^{-1} s^{-1}.[13] The domain size of graphene can be increased via effectively controlling the nuclear density, for instance, methods including chemical mechanical polishing,[14,15] melting copper substrates,[2,5,16] oxygen treatment,[1] and C:H ratio modulation[7,17] have been successfully employed to reduce the nucleation density. At the same time, it is also important to understand where the nucleation sites preside. Typically the main nucleation sites for graphene are located at the imperfections on the copper substrates such as impurities, defects, and grain boundaries.[13,14] As a matter of fact, it is clearly evident that the distribution of certain nanoparticles on the graphene films is consistent with the graphene nucleation sites. Nanoparticles often deposit extensively on the centre area of the graphene domains, especially the multilayer domains; however, the potential impact of nucleation sites on nanoparticles has been barely investigated in the literature.[18-21] Particularly, Han[14] et al. have reported that nanoparticles located at the centre of the graphene domains could serve as the nucleation seeds for graphene growth, and they are also related with layer distribution. A detailed analysis about nanoparticles growth has been provided by Gan[22] et al., which suggests that only nanoparticles with the diameters more than 20 nm and introduced by certain preheating methods could be nucleation seeds for graphene domains. Theoretically, controlling the size and density of the particles with the help of oxygen could effectively reduce the nucleation density, affording a larger domain size. Oxygen is mainly employed to passivate the surface active sites and increase growing rate, which ultimately would result in large-scale graphene domains.[13] In addition, it appears that pre-patterned, seeded growth often leads to a much higher nucleation density.[23] Moreover, it was found that the relatively larger pre-seeded particles would give rise to multilayer graphene.[10] Apparently, the hypothesis proposed by Gan[22] et al is fairly vague, and further investigation to thoroughly understand these results is highly desirable.

In this work, we have discussed the structure of nanoparticles, the correlation between the nanoparticles and the graphene nucleation sites, as well as the graphene layers. The deposition of nanoparticles is similar to the growth of graphene films on copper substrates, thus, under certain circumstances, nanoparticles can be considered as the dynamic reflection of graphene growth.

Experimental

Synthesis of Graphene domains

Graphene domains were grown on copper substrates under atmospheric pressure. Particularly, the high gas flow rate refers to the growing in a large quartz tube, whereas the low gas flow rate refers to the growing on the copper substrates in a small quartz tube with one end sealed, which was also placed in the centre of a large quartz tube. Details of the relative growth parameters were reported in our previous work.[24]

Characterizations

Graphene domains and nanoparticles were imaged by thermal field emission scanning electron microscopy (SEM, LEO-1530). The fluctuation of graphene domains, nanoparticles and copper steps has been determined using atomic force microscope in tapping mode (AFM, Agilent 5100).

Results and Discussion

As illustrated in Figure 1a, it appears that nanoparticles are located exactly in the centre of the graphene domains. Plus, the AFM images in Figure 1b show that nanoparticles have deposited in the centre of the multilayer domains of the continuous graphene films. In Figure 1c, the nanoparticle diameter marked with a green line is about 100 nm, and its height is about 10 nm. However, the size for nanoparticles is not even, and it often varies along with the growing parameters.

We next studied the morphology of nanoparticles prepared, and it appears that several different types are present, for instance, the irregular and separated structure shown in Figure 1d, the circled structure shown in Figure 1e, and the triangle structure shown in Figure 1f. Generally, these nanoparticles don't seem to possess an identical shape, and their composition is also variable. Notably, results obtained from Energy Dispersive X-ray Spectroscopy (EDS) analysis showed that these nanoparticles are composed of silicon, tungsten, and copper, as shown in Figure S1. Theoretically, the copper signal is mainly originated from the substrate used, because nanoparticles should not contain much copper. The peak positions for tungsten and silicon are close, and no tungsten was employed in the preparation process or in the substrates and quartz tube, thus the presence of tungsten could be excluded and the corresponding signal should be assigned to silicon. That said, we conclude these nanoparticles are only composed of silicon. The nanoparticles in the centre of domains are very small, thus the EDS results would not be precise. In order to obtain detailed information about the composition of nanoparticles, large particles on graphene or copper substrates were closely examined, as illustrated in Figure S2 and S3. Interestingly, elements such as O, Fe, Al, Si, Ca, and C have been detected. Based on the complex nanostructure observed in the nanoparticles discussed above, we conclude that these nanoparticles should be multi-element complexes.

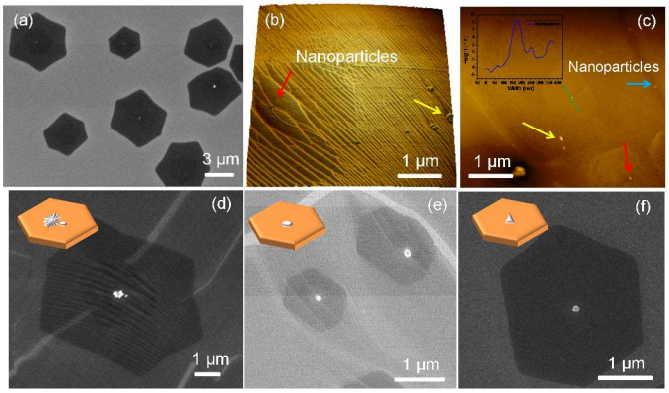

Figure 1. Structure of nanoparticles. (a) SEM image of nanoparticles at the centres of graphene domains; (b,c) AFM images of nanoparticles on graphene; (d-f) SEM images exhibiting different shapes of nanoparticles.

The fact that nanoparticles are presiding in the centre of the graphene domains has indicated that nanoparticles and graphene domains could share common nucleation sites. Therefore, it appears that the active sites on copper substrates not only could promote the deposition of carbon, but also should assist the accumulation of other elements. The locations of nanoparticles can serve as a straightforward reflection for the nucleation sites of graphene.

In order to obtain an accurate distribution of nanoparticles, a statistic analysis was conducted to the image shown in Figure 2a. Specifically, there are about 50 nanoparticles present in the SEM vision field; around 30 nanoparticles are located exactly in the centre of the graphene domains, and the others are presiding on domain edges or copper substrates. Therefore, we conclude that about 60% of the nanoparticles were formed in the domain centre, which has indicated that the locations for graphene domains and nanoparticles are coincidently overlapping.

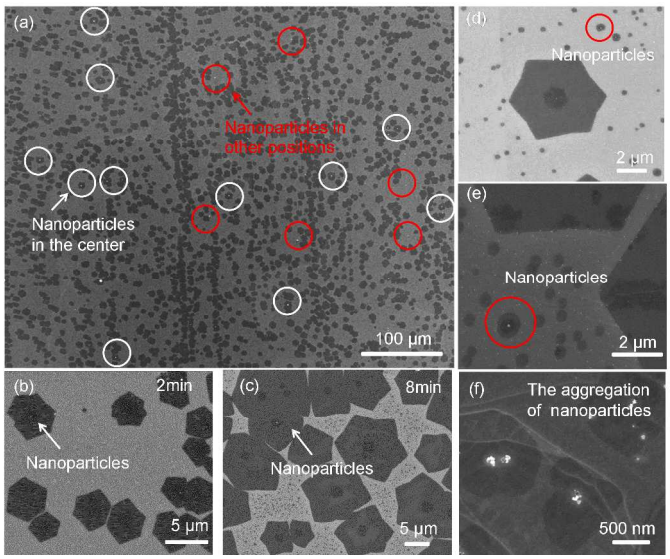

Figure 2. Distribution and size of nanoparticles. (a) Distribution of nanoparticles; Nanoparticles grown for 2 min (b) and 8 min (c); (d) Nanoparticles on different graphene domains; (e) Nanoparticles on graphene nucleus; (f) Aggregation of nanoparticles an the centre of multilayer domains.

We next compared the results illustrated in Figure 2b and Figure 2c, and it turned out that the nanoparticle size did not increase with time, which was different from the graphene domains. In addition, when the graphene domains are still small nucleus, nanoparticles have already been formed on the domain centre, as marked by the red circles in Figure 2d and Figure 2e. Interestingly, it was found that the size of nanoparticles on the small nucleus was close to the ones on the large graphene domains, as shown in Figure 2d. Under particular growing atmosphere, the size of the nanoparticles should be maintained at a certain level.

According to Figure 2b~e, not all the graphene domains have nanoparticles attached. Besides, the attachment of nanoparticles has no connection with the size of graphene domains. Different batches of graphene domains under the same growth parameters could possess different morphology. However, even if the thickness of graphene and the distribution of nanoparticles are different, the size of domains obtained is close to each other, as long as

the growth parameters are maintained the same (Figure S4). Besides, the deposition of Ag particles in Figure S5 demonstrates that the nanoparticles can form later than graphene, and share the same nucleation sites with it. At this stage, evidence shows that nanoparticles are not the nucleus as it has no relationship with the nucleation density of graphene, even though it has been confirmed that graphene domains and nanoparticles share common nucleation sites.

Under low gas flow rate conditions, some of the graphene domains do not have nanoparticles attached, as shown in Figure 2b and c, and the nanoparticles formed seem to be fairly small. On the other hand, when the gas flow rate was increased, the density and size of the nanoparticles were also increased. Notably, nanoparticles only aggregated in the centre of the multilayer graphene domains (Figure 2f), which indicates that the substrates underneath should possess higher attracting ability. The substrates of nanoparticles include copper and graphene domains. Generally, the active sites such as defects and impurities on copper promote the nucleation of graphene domains. Compared with copper substrates, the amplitude, defects, and impurities of graphene can be neglected. Otherwise, nanoparticles should only locate on graphene domains. However, in Figure 2a, the other 40% nanoparticles are distributed on domain edges or copper substrates. Therefore, it is the copper substrate instead of graphene that hinders the diffusion of nanoparticle precursors and generating the formation of nanoparticles.

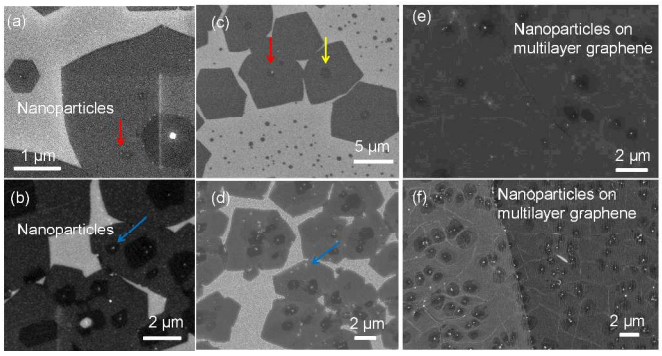

Figure 3. Nanoparticles on multilayer graphene. Distribution of nanoparticles distant from the centre under (a) low and (b) high gas flow rates; Distribution of nanoparticles on graphene domains under low (c) and high (d) gas flow rate conditions; Distribution of nanoparticles on graphene films under (e) low and (f) high gas flow rates.

According to the analysis illustrated in Figure 2a, nanoparticles preferentially adhere to the centre of the graphene domains, however, a portion of them still locates on other sites, especially under high gas flow rate conditions. For example, some nanoparticles preside on the edges of the graphene domains (blue arrow in Figure 1c), single layer parts (yellow arrow in Figures 1b, c), and copper substrates (Figure 1c). With a relatively high SEM magnification rate, the small nanoparticles sitting on the peripheral parts of the graphene domains have been visualized, as shown in Figure 3a. Notably, multilayer graphene marked with a red arrow can be found below the nanoparticles; when the gas flow rate was increased, nanoparticles and multilayer graphene domains were more distinct, as marked with a blue arrow in Figure 3b. Meanwhile, the distribution of nanoparticles is consistent with the multilayer graphene domains, which seems to be similar to Figure 3a. The formation of multilayer graphene on copper substrates has been discussed in detail in several recent reports, which suggest that additional layers mainly grow from the interface of graphene and copper substrates,[19,25] except that the existing monolayer graphene can effectively assisted the growth of the epitaxy.[26,27] Since the multilayer graphene domains grow on copper substrates instead of the graphene surface, the active sites on copper substrates should also play a critical role on the nucleation process.

Nanoparticles should have the same nucleation sites with the multilayer graphene domains, as supported by our experimental results. Comparing Figure 3c (nanoparticles on graphene domains) and Figure 3e (nanoparticles on graphene films) with Figures 3d and 3f respectively, we have found that when the gas flow rate was increased, the concentration of nanoparticles and the coverage the ratio of multilayer graphene domains has increased as well. Herein, the high gas flow rate refers to the growing process directly taking place in a large quartz tube, whereas the low gas flow rate means that samples were kept in an additional small quartz tube with one end sealed. Details about growing conditions have been summarized in the experimental section. The nanoparticle precursors mainly come from the quartz tube, copper substrates, impurities mixed with gases introduced and so on. Theoretically, the small quartz tube not only could reduce the gas flow rate, but also should reduce the amount of nanoparticle precursors. On the other hand, high gas flow rates should lead to high nucleation density in the graphene domains, whereas an excess of precursors would result in high density nanoparticles, as illustrated in Figures 3b, 3d, and 3f. When the gas flow rate was sufficiently high, nanoparticles would deposit on the single layer graphene distant from the centre of graphene domains, as shown in Figure 3d.

As previously reported, the stacking order of graphene domains is not limited to AB bernal for bilayer structures, or ABA for tri-layer structures, instead, twisted structure is very common for multilayer graphene.[18,21,28] In this work, the AB bernal stacking order and twisted order are clearly evident, as demonstrated in Figures 4d and e, respectively. For small nanoparticles in the centre area, these two types of stacking orders are also existent; for instance, the AB stacking order has been found in Figure 4a, and the twisted one is shown in Figure 4b, both marked with red arrows. Generally, if the upper and lower domains have similar shape, common nucleation sites, and their size distinction is not significant, they usually possess the same lattice orientation (Figure 4a). On the contrary, if the size distinction is large, such as the domain pointed by the red arrow in Figure 4b, or if the lower layer is away from the centre, such as the domain pointed by the yellow arrow in Figure 4b, these multilayer graphene domains usually exhibit twisted structure. In addition, it appears that the stacking order of the multilayer graphene domains should not have specific relationship with the growing of nanoparticles.

Subsequently, the graphene domains were transferred to silicon substrates by PMMA, as shown in Figures 4c-e. Notably, only a few nanoparticles were left in the centre of the graphene domains, as indicated by the red arrows in Figure 4c and e. Apparently, the adhesion ability of nanoparticles is not very

high, thus some material has been lost during the process of transferring, which also reflects that the nanoparticles are just sediments locating in the centre of graphene domains instead of nucleation seeds.

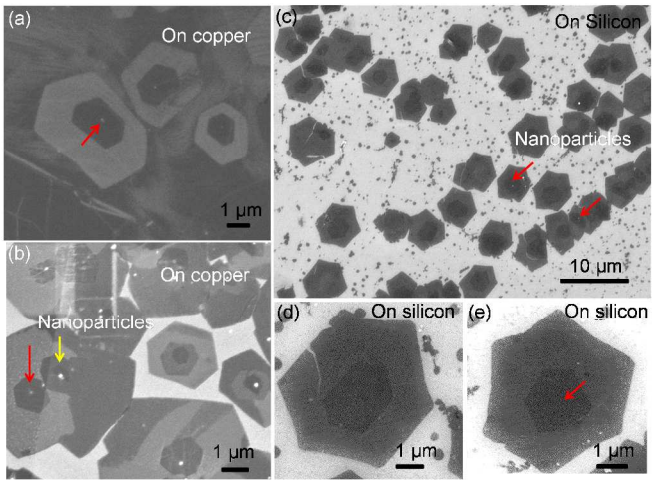

Figure 4. Stacking order of multilayer graphene. (a) The bernal and (b) twisted stacking order of multilayer graphene on copper substrates with nanoparticles; (c) Graphene domains on silicon substrates; (d) The bernal and (e) twisted stacking order of multilayer graphene on silicon substrates.

High hydrogen flow rate is usually used to reduce the nucleation rate and etch graphene to form monolayer domains with regular shape.[7,8,29] In this work, the gas ratio for the high gas flow rate preparation is: CH_4: H_2: Ar = 10: 5: 200, which should lead to high nucleation rate and the formation of large amount of nanoparticles, as shown in Figures 3d and 3f. When hydrogen flow rates were increased (CH_4: H_2: Ar = 2: 200: 0), regular monolayer hexagonal graphene domains were obtained, and no nanoparticle was formed on the surface (Figure 5a). It is known that hydrogen can reduce methane solubility in copper,[29,30] leading to a low growing velocity of graphene, which should also be applicable to nanoparticles. Therefore, almost no nanoparticles were found on the graphene domains under high hydrogen flow rate conditions, similar to other examples reported.[7,8]

Based on the discussions mentioned above, the attachment of the nanoparticles and the formation of multilayer graphene are mainly due to the active sites on copper substrates. In order to verify this inference, growth on melted copper substrates was introduced. When the copper substrates are molten, impurities can dissolve into the copper material. At the same time, defects such as steps and grain boundaries would also disappear, affording large-scale monolayer graphene domains retaining no nanoparticles, as shown in Figure 5b. On the contrary, the impurities and other defects can't be eliminated on solid copper substrates. When graphene was grown on solid copper substrates with the same growth parameters except the temperature, continuous multilayer graphene films can be synthesized and nanoparticles located in the centre of multilayer parts (inset in Figure 5b).

The schematic diagram in Figure 5c describes the deposition mechanism for the nanoparticles in four representative cases, including the ones grown on rough copper surface, copper with impurities, melting copper, and under high hydrogen flow rate. It's well known that the rough copper surface can promote the nucleation of graphene, and the nucleation density of graphene can be reduced by substrate polishing.[14] When carbon species encounter the protrusion or depression areas on copper substrates, nucleation process is initiated and the growth will start. Besides, both carbon species and nanoparticles formed can be trapped on the rough sites, as shown in the first picture of Figure 5c. Moreover, the rough topography of copper substrates can also help the diffusion of carbon species underneath the monolayer graphene, eventually forming multilayer ones.[14] Because the carbon concentration below the upper layer graphene is often low, most of the lower layer domains are much smaller than the upper layer,[25] even though these two layers share the same nucleation sites. At the same time, the movement of copper substrates can be hampered by graphene films, especially in multilayer parts, which would result in wide steps in multilayer graphene, as previously reported by our laboratory.[31] Impurities such as copper oxide[22] can provide heterogeneous nucleation sites for the growing of graphene and the nanoparticles (the second picture in Figure 5c). To the contrast, because hydrogen has exhibited higher diffusion and combination ability than carbon on the copper substrates, it can largely reduce the nucleation density and effectively etch graphene. Therefore, pure monolayer high-quality graphene films can be produced under high hydrogen flow conditions, as shown in the third picture of Figure 5c. Theoretically, melting can cure the imperfections on copper substrates such as impurities, coarse morphology and steps, which should assist the growth of monolayer graphene without the formation of nanoparticles (the fourth picture in Figure 5c).

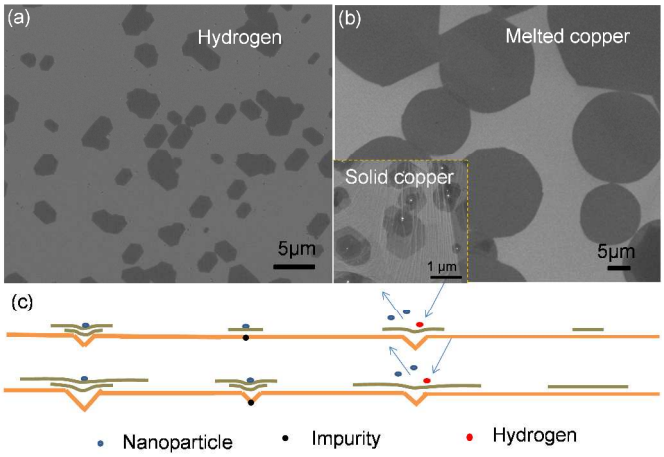

Figure 5. Clean graphene domains without nanoparticles and the schematic diagram for the formation of nanoparticles. (a) Graphene domains grown under high hydrogen flow rate conditions; (b) Graphene domains grown on melted copper substrates, inset: graphene domains grown on solid copper substrates; (c) Schematic diagram for the formation of nanoparticles.

When the gas flow rate is low (growth in the small quartz tube), graphene domains tend to nucleate dispersively on copper substrates, as demonstrated in Figure 6a. The domain size is relatively big and the domain shape is more regular. Such nucleation process is mainly due to the fact that imperfections on copper substrates are uniformly distributed. Meanwhile, the step edges of copper can also provide nucleation sites for graphene formation.[31,32] Under high gas flow rate (growth in the large quartz tube), such growth mechanism can be realized. Graphene domains nucleating near the step edges are smaller and the shape is irregular in Figure 6b. Copper steps are often distorted, presumably due to the material imperfections and graphene formed on their surface, which makes graphene domains arranging along curves, as illustrated in Figure 6b. When the gas flow rate is increased, there would be more nanoparticles on the graphene domains, as shown in Figure 6b, and the distribution of nanoparticles is more complex compared with that in Figure 6a. However, nanoparticles also tend to position themselves in the centre of the multilayer domains in Figure 6b. The step width in Figure 6c marked with red and blue lines is different, as shown in Figure 6d. These results are possibly related to the distribution of the monolayer and multilayer graphene. Plus, it was reported that wide steps often yielded multilayer graphene domains, whereas narrow steps generally led to monolayer graphene films.[31] Therefore, we conclude that the graphene under the red line should be multi-layered, whereas the graphene below the blue line should be mono-layered. Hence in Figure 6c, nanoparticles indicated by arrows should be formed in the centre of the multilayer parts, although most of the multilayer parts are on the peripheral parts of the monolayer domains. We conclude that under step-driven growth mechanism, nanoparticles also share common nucleation sites with the multilayer graphene.

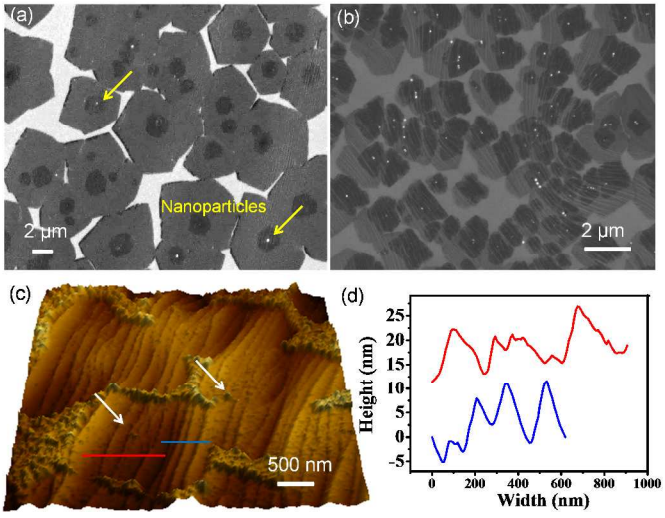

Figure 6. Two growth modes of graphene domains. (a) Imperfection-driven and (b) step-driven growth of graphene domains; (c) AFM image of graphene domains; (d) Height profiles.

Conclusions

In summary, we have found that the nanoparticles prepared are sediment-like material, similar to the graphene films deposited on the copper substrates. Interestingly, it appears that nanoparticles and graphene domains share common nucleation sites. Besides, the distribution of nanoparticles is consistent with the growing of multilayer graphene. The structure, size and composition of the nanoparticles are variable, depending on the components and concentrations of precursors. As a matter of fact, it turned out that high concentrations of precursors would result in nanoparticles with higher density and larger diameters. However, it seems the size of the nanoparticles does not increase with the growing time. Plus, there is no obvious relationship between the stacking order of multilayer graphene and nanoparticles. Under high hydrogen flow rate conditions, or on melting copper substrates, no nanoparticle was formed. Our efforts to understand the deposition mechanism of nanoparticles should greatly facilitate the analysis of nucleation mechanism, which possibly could afford ideal approach to control the number of graphene layers.

Acknowledgements

This work is supported by National Science Foundation of China (51372133), Beijing Science and Technology Program (D141100000514001), National Program on Key Basic Research Project (2011CB013000), Tsinghua University Initiative Scientific Research Program (2012Z02102).

Notes

[a]*School of Materials Science and Engineering, State Key Laboratory of New Ceramics and Fine Processing, Key Laboratory of Materials Processing Technology of MOE, Tsinghua University, Beijing 100084, P. R. China. E-mail: hongweizhu@tsinghua.edu.cn*

[b]*Department of Mechanical Engineering, Tsinghua University, Beijing 100084, P. R. China*

[c]*Centre for Nano and Micro Mechanics, Tsinghua University, Beijing 100084, P. R. China*

† Electronic Supplementary Information (ESI) available. See DOI: 10.1039/b000000x/

References

1 H. L. Zhou, W. J. Yu, L. X. Liu, R. Cheng, Y. Chen, X. Q. Huang, Y. Liu, Y. Wang, Y. Huang and X. F. Duan, *Nat. Commun.*, 2013, **4**, 2096.

2 A. Mohsin, L. Liu, P. Z. Liu, W. Deng, I. N. Ivanov, G. L. Li, O. E. Dyck, G. Duscher, J. R. Dunlap, K. Xiao and G. Gu, *ACS Nano*, 2013, **7**, 8924.

3 T. R. Wu, G. Q. Ding, H. L. Shen, H. M. Wang, L. Sun, D. Jiang, X. M. Xie and M. H. Jiang, *Adv. Funct. Mater.*, 2013, **23**, 198.

4 Y. H. Zhang, Z. Y. Chen, B. Wang, Y. W. Wu, Z. Jin, X. Y. Liu and G. H. Yu, *Mater. Lett.*, 2013, **96**, 149.

5 D. C. Geng, B. Wu, Y. L. Guo, L. P. Huang, Y. Z. Xue, J. Y. Chen, G. Yu, L. Jiang, W. P. Hu and Y. Q. Liu, *P. Natl. Acad. Sci. Usa.*, 2012, **109**, 7992.

6 Z. Yan, J. Lin, Z. W. Peng, Z. Z. Sun, Y. Zhu, L. Li, C. S. Xiang, E. L. Samuel, C. Kittrell and J. M. Tour, *ACS Nano*, 2013, **7**, 2872.
7 H. Wang, G. Z. Wang, P. F. Bao, S. L. Yang, W. Zhu, X. Xie and W. J. Zhang, *J. Am. Chem. Soc.*, 2012, **134**, 18476.
8 L. B. Gao, W. C. Ren, H. L. Xu, L. Jin, Z. X. Wang, T. Ma, L. P. Ma, Z. Y. Zhang, Q. Fu, L. M. Peng, X. H. Bao and H. M. Cheng, *Nat. Commun.*, 2012, **3**, 699.
9 X. S. Li, C. W. Magnuson, A. Venugopal, R. M. Tromp, J. B. Hannon, E. M. Vogel, L. Colombo and R. S. Ruoff, *J. Am. Chem. Soc.*, 2011, **133**, 2816.
10 W. Wu, L. A. Jauregui, Z. H. Su, Z. H. Liu, J. M. Bao, Y. P. Chen and Q. K. Yu, *Adv. Mater.*, 2011, **23**, 4898.
11 A. W. Tsen, L. Brown, M. P. Levendorf, F. Ghahari, P. Y. Huang, R. W. Havener, C. S. Ruiz-Vargas, D. A. Muller, P. Kim and J. Park, *Science*, 2012, **336**, 1143.
12 G. H. Lee, R. C. Cooper, S. J. An, S. Lee, A. van der Zande, N. Petrone, A. G. Hammerherg, C. Lee, B. Crawford, W. Oliver, J. W. Kysar and J. Hone, *Science*, 2013, **340**, 1073.
13 Y. F. Hao, M. S. Bharathi, L. Wang, Y. Y. Liu, H. Chen, S. Nie, X. H. Wang, H. Chou, C. Tan, B. Fallahazad, H. Ramanarayan, C. W. Magnuson, E. Tutuc, B. I. Yakobson, K. F. McCarty, Y. W. Zhang, P. Kim, J. Hone, L. Colombo and R. S. Ruoff, *Science*, 2013, **342**, 720.
14 G. H. Han, F. Gunes, J. J. Bae, E. S. Kim, S. J. Chae, H. J. Shin, J. Y. Choi, D. Pribat and Y. H. Lee, *Nano Lett.*, 2011, **11**, 4144.
15 Z. T. Luo, Y. Lu, D. W. Singer, M. E. Berck, L. A. Somers, B. R. Goldsmith and A. Johnson, *Chem. Mater.*, 2011, **23**, 1441.
16 Y. Wu, Y. Fan, S. Speller, G. L. Creeth, J. T. Sadowski, K. He, A. W. Robertson, C. S. Allen and J. H. Warner, *ACS Nano*, 2012, **6**, 5010.
17 X. S. Li, C. W. Magnuson, A. Venugopal, J. H. An, J. W. Suk, B. Y. Han, M. Borysiak, W. W. Cai, A. Velamakanni, Y. W. Zhu, L. F. Fu, E. M. Vogel, E. Voelkl, L. Colombo and R. S. Ruoff, *Nano Lett.*, 2010, **10**, 4328.
18 B. Wu, D. C. Geng, Y. L. Guo, L. P. Huang, Y. Z. Xue, J. Zheng, J. Y. Chen, G. Yu, Y. Q. Liu, L. Jiang and W. P. Hu, *Adv. Mater.*, 2011, **23**, 3522.
19 S. Nie, W. Wu, S. R. Xing, Q. K. Yu, J. M. Bao, S. S. Pei and K. F. McCarty, *New J. Phys.*, 2012, **14**, 093028.
20 A. W. Tsen, L. Brown, R. W. Havener and J. Park, *Accounts Chem. Res.*, 2013, **46**, 2286.
21 C. C. Lu, Y. C. Lin, Z. Liu, C. H. Yeh, K. Suenaga and P. W. Chiu, *ACS Nano*, 2013, **7**, 2587.
22 L. Gan and Z. T. Luo, *ACS Nano*, 2013, **7**, 9480.
23 Q. K. Yu, L. A. Jauregui, W. Wu, R. Colby, J. F. Tian, Z. H. Su, H. L. Cao, Z. H. Liu, D. Pandey, D. G. Wei, T. F. Chung, P. Peng, N. P. Guisinger, E. A. Stach, J. M. Bao, S. S. Pei and Y. P. Chen, *Nat. Mater.*, 2011, **10**, 443.
24 L. L. Fan, Z. Li, X. Li, K. L. Wang, M. L. Zhong, J. Q. Wei, D. H. Wu and H. W. Zhu, *Nanoscale*, 2011, **3**, 4946.
25 Q. Y. Li, H. Chou, J. H. Zhong, J. Y. Liu, A. Dolocan, J. Y. Zhang, Y. H. Zhou, R. S. Ruoff, S. S. Chen and W. W. Cai, *Nano Lett.*, 2013, **13**, 486.
26 K. Yan, H. L. Peng, Y. Zhou, H. Li and Z. F. Liu, *Nano Lett.*, 2011, **11**, 1106.
27 L. X. Liu, H. L. Zhou, R. Cheng, W. J. Yu, Y. Liu, Y. Chen, J. Shaw, X. Zhong, Y. Huang and X. F. Duan, *ACS Nano*, 2012, **6**, 8241.
28 L. Brown, R. Hovden, P. Huang, M. Wojcik, D. A. Muller and J. Park, *Nano Lett.*, 2012, **12**, 1609.
29 I. Vlassiouk, M. Regmi, P. F. Fulvio, S. Dai, P. Datskos, G. Eres and S. Smirnov, *ACS Nano*, 2011, **5**, 6069.
30 M. Losurdo, M. M. Giangregorio, P. Capezzuto, G. Bruno, *Phys. Chem. Chem. Phys.*, 2011, **13**, 20836.
31 L. L. Fan, Z. Li, Z. P. Xu, K. L. Wang, J. Q. Wei, X. Li, J. Zou, D. H. Wu and H. W. Zhu, *AIP Adv.*, 2011, **1**, 0321453.
32 K. Hayashi, S. Sato and N. Yokoyama, *Nanotechnol.*, 2013, **24**, 0256032.

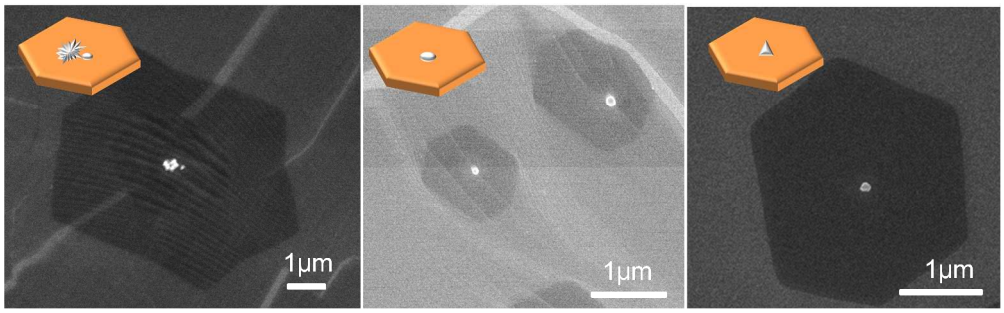

The location of nanoparticles is a straightforward reflection for the nucleation sites of graphene growth. The deposition of the nanoparticles is consistent with the distribution of multilayer graphene.